

**Analytical model for thermal boundary conductance and equilibrium thermal accommodation coefficient at solid/gas interfaces**

Ashutosh Giri and Patrick E. Hopkins

Citation: *The Journal of Chemical Physics* **144**, 084705 (2016); doi: 10.1063/1.4942432

View online: <http://dx.doi.org/10.1063/1.4942432>

View Table of Contents: <http://scitation.aip.org/content/aip/journal/jcp/144/8?ver=pdfcov>

Published by the [AIP Publishing](#)

---

**Articles you may be interested in**

[Measurement of thermal accommodation coefficients using a simplified system in a concentric sphere shells configuration](#)

*J. Vac. Sci. Technol. A* **32**, 061602 (2014); 10.1116/1.4901011

[Graphics processing unit \(GPU\)-based computation of heat conduction in thermally anisotropic solids](#)

*AIP Conf. Proc.* **1511**, 1401 (2013); 10.1063/1.4789206

[Pressure dependency of thermal boundary conductance of carbon nanotube/silicon interface: A molecular dynamics study](#)

*J. Appl. Phys.* **112**, 053501 (2012); 10.1063/1.4749798

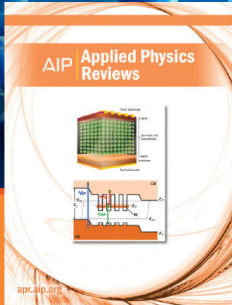
[Molecular Boundary Conditions and Accommodation Coefficient on A Nonequilibrium Liquid Surface](#)

*AIP Conf. Proc.* **1333**, 859 (2011); 10.1063/1.3562753

[An experimental assembly for precise measurement of thermal accommodation coefficients](#)

*Rev. Sci. Instrum.* **82**, 035120 (2011); 10.1063/1.3571269

---



**NEW Special Topic Sections**

**NOW ONLINE**  
Lithium Niobate Properties and Applications:  
Reviews of Emerging Trends

**AIP** | Applied Physics  
Reviews

# Analytical model for thermal boundary conductance and equilibrium thermal accommodation coefficient at solid/gas interfaces

Ashutosh Giri and Patrick E. Hopkins

Department of Mechanical and Aerospace Engineering, University of Virginia, Charlottesville, Virginia 22904, USA

(Received 7 January 2016; accepted 9 February 2016; published online 25 February 2016)

We develop an analytical model for the thermal boundary conductance between a solid and a gas. By considering the thermal fluxes in the solid and the gas, we describe the transmission of energy across the solid/gas interface with diffuse mismatch theory. From the predicted thermal boundary conductances across solid/gas interfaces, the equilibrium thermal accommodation coefficient is determined and compared to predictions from molecular dynamics simulations on the model solid-gas systems. We show that our model is applicable for modeling the thermal accommodation of gases on solid surfaces at non-cryogenic temperatures and relatively strong solid-gas interactions ( $\varepsilon_{sf} \gtrsim k_B T$ ). © 2016 AIP Publishing LLC. [<http://dx.doi.org/10.1063/1.4942432>]

## I. INTRODUCTION

Condensation, evaporation, and thermal transport processes of a working fluid underlie critical physical mechanisms in a wide variety of technologies used for energy conversion such as low grade waste heat recovery,<sup>1,2</sup> geothermal energy harvesting,<sup>3,4</sup> heat pipe engineering and thermal ground plane development,<sup>5-7</sup> sea water energy conversion,<sup>8,9</sup> and heat dissipation in nanoscale electronics.<sup>10</sup> In these applications, the energy exchange mechanisms are governed by the microscopic kinetics between the molecules in the fluid and those on a solid surface, or the solid surface itself. Therefore, a coupled understanding of both mass and thermal transport is necessary for a complete description of heat exchange at solid/vapor interfaces.

At the microscopic level, the efficiency of interfacial energy exchange is quantified by the Kapitza conductance,  $h_K$  that relates the heat flux to the temperature drop at the interface. Although the Kapitza conductance between crystalline solids has been extensively studied, there has been relatively far less progress in the fundamental understanding of solid/gas interfaces. For example, analytical descriptions of  $h_K$  across solid/gas interfaces has been limited to cryogenic temperatures,<sup>11-13</sup> whereas the theoretical models for  $h_K$  across solid/solid interfaces are able to describe the physics at non-cryogenic temperatures as well (including scenarios of variable bonding at the interface, material anisotropy, and anharmonic interactions at the interface) through the widely used Diffuse Mismatch Model (DMM) and Acoustic Mismatch Model (AMM).<sup>14-18</sup> Moreover, the mass effect for energy exchange due to gas atoms colliding at a solid surface has been limited to simplistic models such as the hard sphere model,<sup>19</sup> which does not take into consideration the energy states in the solid as well as the interaction strength between the solid surface and the gas atoms.<sup>20-22</sup> Although Goodman and Wachman have derived an analytical expression to describe the efficiency of energy exchange at solid/gas interfaces that is applicable at non-cryogenic

temperatures, their closed form model is semi-empirical in nature and needs certain properties of the experimental data.<sup>23</sup>

Recent studies have explored the effect of gas molecular mass and interfacial bonding on heat transport via molecular dynamics (MD) simulations, lending important physical insight into the solid-gas energy exchange dynamics.<sup>20-22,24,25</sup> Liang *et al.*<sup>20,21</sup> have compared their results to the hard-sphere model and demonstrated the failure of this model to capture the nanoscale heat transfer exchange dynamics at solid/gas interfaces. Therefore, the goal of this current work is to derive a microscopic model that relates  $h_K$  at a solid-gas interface beyond the hard sphere model and is applicable at non-cryogenic temperatures. We compare our model predictions to results from MD simulations on specific solid-gas systems.

## II. DIFFUSE MISMATCH MODEL FOR SOLID/GAS INTERFACES

For a gas molecule colliding at a gas/solid interface, the efficiency of energy exchange is described in terms of an equilibrium thermal accommodation coefficient,

$$\alpha_T(E) = \lim_{\Delta T \rightarrow 0} \frac{E'_g - E_g}{E_g - E_s}, \quad (1)$$

where  $E_g$  is the energy of the gas,  $E'_g$  is the energy of the gas leaving the surface, and  $E_s$  is the energy of the solid. We retain the functionality of the accommodation coefficient with energy to be consistent with our phonon/gas molecule energy transmission in the theoretical development presented here. From classical gas dynamics, in the temperature jump regime  $0.01 \leq Kn \leq 0.1$  (where  $Kn$  is the Knudsen number), the thermal boundary conductance from a solid to a gas is given by<sup>19</sup>

$$h_K = \frac{F k_B I \alpha_T}{2 - \alpha_T}, \quad (2)$$

where  $F = 4$  for a monoatomic gas and  $F = 6$  for a diatomic gas,  $k_B$  is the Boltzmann constant, and  $I$  is the collision rate per unit area. Examining Eq. (2) qualitatively, we find that this thermal boundary conductance can be described by a power flux ( $Fk_B I$ ) that is partially transmitted across the interface, dictated by a “transmission” term,  $\zeta$ , that is related to  $\alpha_T$ . Therefore, from inspection, the energy transmission from the gas to the solid is given by

$$\zeta_{g \rightarrow s} = \frac{\alpha_T}{2 - \alpha_T} \rightarrow \alpha_T = \frac{2\zeta_{g \rightarrow s}}{1 + \zeta_{g \rightarrow s}}, \quad (3)$$

where the subscripts “g” and “s” refer to the gas and solid, respectively. Equation (3) gives a direct relationship between a typical interfacial transmission coefficient, which can be calculated via computational methods or analytical models (such as, for example, the DMM),<sup>14</sup> and the thermal accommodation coefficient. Using this relationship, in the remainder of this work, we will derive  $\alpha_T$  by considering the transmission of energy between phonons in a solid and an interacting gas.

From semi-classical theory, the phonon thermal flux in an isotropic solid is given by<sup>26</sup>

$$q_s = \frac{1}{4} \sum_j \int_0^{\omega_{\max,j}} \hbar \omega D_j(\omega) f_{BE} v_j d\omega, \quad (4)$$

where  $\hbar$  is the reduced Planck’s constant,  $D$  is the phonon density of states,  $f_{BE}$  is the Bose-Einstein distribution function,  $v$  is the phonon velocity, and  $j$  refers to the phonon polarization. Assuming equilibrium conditions at the interface, which is the focus of this work, as our aim is to develop an analytical model of the equilibrium thermal accommodation coefficient, the thermal boundary conductance between the solid and the accommodating gas is given by

$$h_K = \frac{1}{4} \sum_j \int_0^{\omega_{\max,j}} \hbar \omega D_j(\omega) \frac{\partial f_{BE}}{\partial T} v_j \zeta_{s \rightarrow g} d\omega, \quad (5)$$

where  $T$  is the temperature at the interface (assumed, in this work, to be in equilibrium). This expression for thermal boundary conductance determines the interfacial transport by examining the partial transmission of phonon energy into the gas. We have detailed this specific derivation for phonon thermal boundary conductance in our previous works.<sup>27,28</sup>

Since equilibrium is assumed between the solid and the gas, Eq. (5) is mathematically equivalent to the thermal boundary conductance determined from considering a thermal flux of gas molecules transferring energy to the phonons. The thermal boundary conductance from the gas to the solid is given by

$$h_K = \int_{\varepsilon} F \varepsilon \frac{\partial I_{\varepsilon}}{\partial T} \zeta_{g \rightarrow s} d\varepsilon, \quad (6)$$

where  $I_{\varepsilon}$  is the spectral collision frequency and  $\int I_{\varepsilon} d\varepsilon = I$ , where  $I$  is defined from Eq. (2). The spectral nature of Eq. (2) comes from the velocity distribution of gas molecules so that from Kinetic Theory,<sup>29</sup> the spectral collision frequency per

unit area of an isotropic flux of gas molecules impinging upon a solid surface is given by<sup>23</sup>

$$I_c d\phi d\theta dc = \frac{n}{2\pi} \left( \frac{m}{k_B T} \right)^2 c^4 \exp \left[ -\frac{mc^2}{2k_B T} \right] \sin[2\theta] d\phi d\theta dc, \quad (7)$$

where  $n$  and  $c$  are the number density and speed of the gas molecules, respectively. Equation (7) is derived from the definition of a Maxwellian stream of atoms, and it is important to note that the stream properties of a gas approaching a surface are not the same as the properties of a gas in equilibrium.<sup>19</sup> Given that  $c = \sqrt{2\varepsilon/m}$ , the collision rate per unit energy on the solid surface is

$$I_{\varepsilon} d\phi d\theta d\varepsilon = \frac{2}{\pi} \frac{n}{m} \left( \frac{\varepsilon}{k_B T} \right)^2 \left( \frac{2\varepsilon}{m} \right)^{-\frac{1}{2}} \times \exp \left[ -\frac{\varepsilon}{k_B T} \right] \sin[2\theta] d\phi d\theta d\varepsilon, \quad (8)$$

where  $n = P/(k_B T)$ , where  $P$  is the pressure. To parallel the phonon thermal flux mathematically described in Eq. (4), the thermal fluxes from the gas molecules impinging on the solid interface is given by

$$q_g = \int_0^{2\pi} d\phi \int_0^{\pi/2} \sin[2\theta] d\theta \int_0^{\infty} \varepsilon I_{\varepsilon} d\varepsilon, \quad (9)$$

for the case of a monoatomic molecular thermal flux.

To compare typical gas and phononic power fluxes incident on a surface, we plot the phonon thermal flux in Au determined via Eq. (4) and the elemental thermal fluxes in He and Xe gases at two different pressures (0.1 and 10 MPa) determined via Eq. (9) as a function of temperature in Fig. 1. For the Au phononic flux calculations, we assume a sine-type phonon dispersion in an isotropic Brillouin zone with maximum phonon frequencies taken as those in the

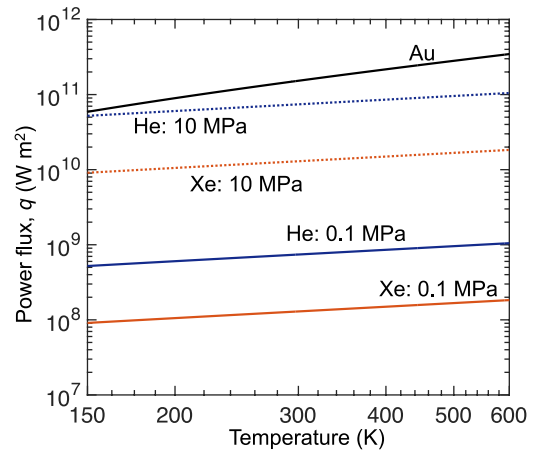


FIG. 1. Power flux as a function of temperature. The power flux for the gold phonons is calculated with Eq. (4) where the power fluxes for the various gasses at the different pressures are calculated with Eq. (9). The power flux of Au phonons incident on an interface can be orders of magnitude greater than the gas power flux incident on an interface, depending on the pressure. Via energy conservation considerations discussed below, this has direct implications on the energy transmission across a solid/gas interface and on the equilibrium thermal accommodation coefficient.

$\Gamma \rightarrow X$  direction.<sup>30</sup> The power flux of Au phonons incident on an interface can be orders of magnitude greater than the gas power flux incident on an interface, depending on the pressure. From the energy conservation considerations discussed below, this has direct implications on the energy transmission across a solid/gas interface and on the equilibrium thermal accommodation coefficient.

Where the calculations of these phonon and molecular thermal fluxes only require knowledge of phonon dispersion and molecular species and densities, respectively, the challenge in predicting the thermal boundary conductance across a solid/gas interface is determining the energy transmission. With knowledge of the transmission coefficient and assuming diffusive scattering, Eq. (3) can be used to determine the equilibrium thermal accommodation coefficient,  $\alpha_T$ . Through the use of diffuse mismatch theory, we present an avenue to predict  $\alpha_T$ , assuming diffusive scattering of the gas molecules and a local equilibrium at the solid/gas interface.

We begin by considering the thermal conductance between a solid surface and a non-condensing gas. In this case, the energy transmission from the solid to the gas,  $\zeta_{s \rightarrow g}$ , is directly related to the energy transmission from the gas to the solid through

$$\zeta_{g \rightarrow s} = 1 - \zeta_{s \rightarrow g}. \quad (10)$$

Equation (10) also ensures diffusive scattering at the solid/gas interface, which is a fundamental assumption of the DMM that is adopted in this work. This assumption implies that the incident energy carriers lose all memory of their initial direction and polarization (in the case of the solid) after scattering at the interface. Now, by invoking the principle of detailed balance,<sup>28,31</sup> which assumes that the solid and the gas are in thermal equilibrium at the interface, the transmission coefficient across the solid/gas interface is given as

$$\zeta_{s \rightarrow g} = \frac{q_g}{q_g + q_s}. \quad (11)$$

To begin to validate our model, the theoretical calculations of  $\zeta_{g \rightarrow s}$  (and consequently the  $\alpha_T$  from Eq. (3)) are carried out for a model Lennard-Jones (LJ) solid that is in contact with a LJ gas. This allows our theoretical predictions to be compared to predictions using MD simulations on these model structures, as described in Sec. III.

### III. MOLECULAR DYNAMICS SIMULATIONS ON SOLID/GAS SYSTEMS

For our MD simulations, we employ the 6-12 Lennard-Jones (LJ) potential,  $U(r) = 4\epsilon[(\sigma/r)^{12} - (\sigma/r)^6]$ , where  $U$  is the interatomic potential,  $r$  is the interatomic separation, and  $\sigma$  and  $\epsilon$  are the LJ length and energy parameters, respectively. The energy parameter in the solid is described by  $\epsilon_{ss} = 0.0503$  eV, while the energy parameter for the gas is modeled to mimic that of Argon ( $\epsilon_{ff} = 0.0103$  eV). The length parameter  $\sigma$  is set to 3.405 Å for both solid and gas interactions. To define the interaction between the solid and gas atoms, we use the Lorentz-Berthelot rule, where the energy

and length parameters for the different species are defined as  $\epsilon_{sf} = \sqrt{\epsilon_{ss}\epsilon_{ff}}$  and  $\sigma_{sf} = (\sigma_{ss} + \sigma_{ff})/2$ , respectively. This is a good approximation for interatomic potentials defined by the same pair potential and also has been used to define the interaction between LJ-based solid/solid as well as solid/gas systems.<sup>32–35</sup> For computational efficiency, the cutoff distance for the interatomic potential is set to  $2.5\sigma$ . We note that, unlike in LJ-based solid/solid interfaces,<sup>36</sup> increasing the cutoff distance by 30% did not result in a statistical change in the MD-predicted  $h_K$ . The mass of the solid is set at 120 atomic mass units (amu) while the mass of the gas is varied in our simulations. A time step of 0.5 fs is used throughout the simulations and the solid-gas system is allowed to equilibrate at 300 K temperature and 10 bars pressure with periodic boundary conditions in all three directions. The equilibration of the solid-gas system is carried out for a total of  $4 \times 10^6$  time-steps under the Nose-Hoover thermostat<sup>37</sup> (constant NVT) and the pressure is controlled via the Berendsen barostat.<sup>38</sup> The equilibrated simulation cell is shown in the top panel of Fig. 2(a).

To calculate  $h_K$  across the solid-gas interface, we use the nonequilibrium MD (NEMD) approach, where a steady heat flux is applied across the simulation domain and the resulting temperature gradient is calculated along the direction of the heat flux. For the subsequent NEMD simulations, the global thermostat is removed and the simulations are conducted under the micro-canonical ensemble (constant NVE) with a heat flux of  $\sim 13$  MW/m<sup>2</sup> by the

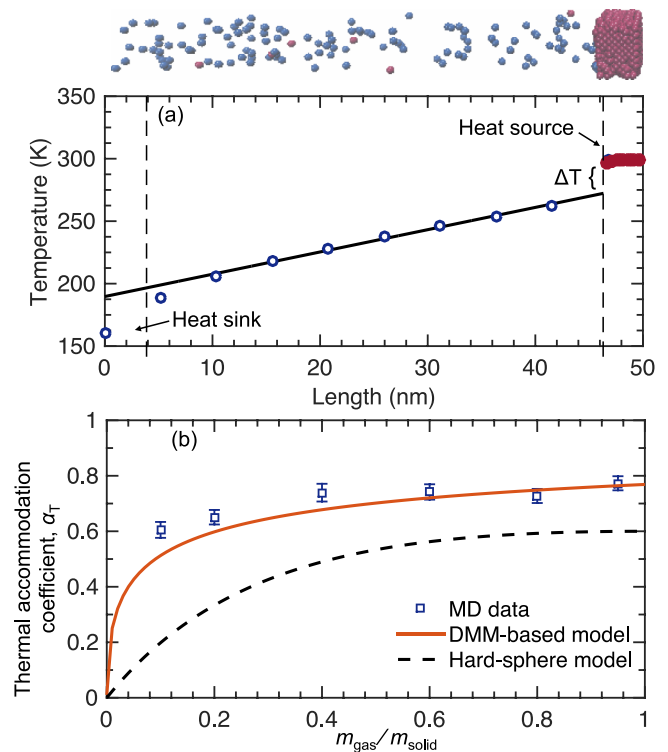


FIG. 2. (a) Top panel: a snapshot of an equilibrated solid/gas model structure. Due to symmetry, only half of the simulation cell is shown. Bottom panel: the temperature response of the Lennard-Jones systems after a steady heat flux is imposed. (b) Thermal accommodation coefficient as a function of mass ratio between the Lennard-Jones systems. Also plotted are the predictions from the hard-sphere model (dashed line) and our DMM-based model (solid line).

Muller-Plathe method.<sup>39</sup> Consequently, we can obtain  $h_K$  from the temperature drop,  $\Delta T$ , at the interface as shown in Fig. 2(a).

With the knowledge of  $h_K$ , we can determine the MD-predicted  $\alpha_T$  from a more detailed form of Eq. (2),

$$h_K = \frac{F k_B \alpha_T P}{(2 - \alpha_T) \sqrt{2\pi m k_B T}}, \quad (12)$$

where  $F = 4$  for a monoatomic gas.<sup>19,22</sup> The predictions are shown in Fig. 2(b) as a function of the mass ratio of gas to solid atom,  $\mu$ . Figure 2(b) also shows the theoretically predicted  $\alpha_T$  for the LJ-based models along with the predictions from the hard-sphere model ( $\alpha_T = 2.4\mu/(1 + \mu)^2$ ). Our theoretical model demonstrates qualitative agreement with the MD results, whereas the predictions from the hard sphere model underestimate the results from the MD simulations, similar to the findings in Ref. 22. Contrary to the hard-sphere model, the sudden decrease of  $\alpha_T$  at relatively low mass ratios predicted by our DMM-based model is also consistent with  $\alpha_T$  predicted via NEMD simulations,<sup>22</sup> further demonstrating the applicability of our model in describing energy transport across solid/gas interfaces. Note, we have used a classical distribution function ( $f = 1/\exp[\hbar\omega/(k_B T)]$ ) in Eq. (5) to model the LJ solid in our analytical calculations in order to directly compare to the MD data in Fig. 2.

The calculations for thermal accommodation in Fig. 2 predict that any gas particle that strikes the solid interface will transfer energy. In other words, if a molecule *can* transfer energy to the solid, it *will*; note, this is a standard, and often restrictive assumption of the DMM and does not take into consideration the strength of interaction between the solid and the gas, which has been shown to control the heat transfer mechanisms across solid/gas interfaces.<sup>20,22</sup> Via MD simulations, Liang *et al.*<sup>20</sup> have shown that  $\alpha_T$  increases with increasing interaction strength between the solid and gas atoms, which reaches its maximum value (of  $h_K$  and consequently  $\alpha_T$ ) at bond strengths of  $\varepsilon_{sf} \gtrsim k_B T$ . While the efficiency of thermal transport across solid/solid interfaces is usually thought to be driven by the relative vibrational spectrums of the constituent crystals, the bond strength dependent  $\alpha_T$  for solid/gas interfaces suggests that the energy transport across these interfaces is significantly dependent on the interfacial properties. In Fig. 3, we show the results of MD simulations from Ref. 22 for variably bonded Au/LJ-Ar systems along with our DMM-based model prediction for a Au/Ar interface. Our model shows appreciable agreement with the MD results for the case when the solid-gas interaction is relatively strong ( $\varepsilon_{sf} \sim k_B T$ ), whereas, the model overpredicts  $\alpha_T$  for the cases with solid-gas interaction energies that are relatively lower than  $k_B T$ . This suggests that our model is not applicable to weakly bonded solid/gas interfaces; we note that this general lack of applicability of any DMM to weakly bonded interfaces is common. However, our model is able to capture the general trend in the MD-predicted  $\alpha_T$  as a function of mass ratio unlike the hard-sphere model which shows a monotonically increasing  $\alpha_T$ . For weakly bonded systems, computational studies have demonstrated that the local vibrational density of states near the interface shows

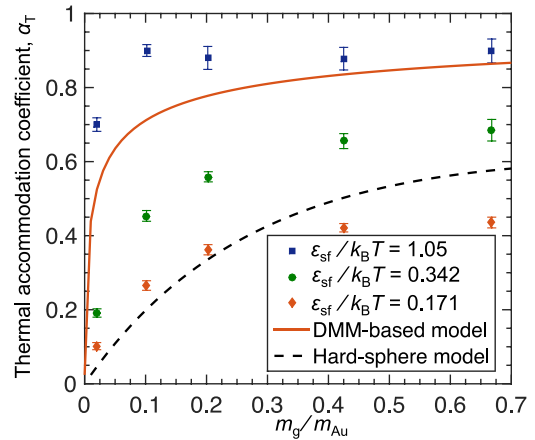


FIG. 3. Thermal accommodation coefficient between Au and LJ gas predicted via the DMM-based model as a function of mass ratio. Also plotted for comparison are the MD-predicted thermal accommodation coefficients at varying solid-gas interaction strengths from Ref. 22 and the prediction from the hard-sphere model.

a linear dependence at relatively low frequencies, which is characteristic to two-dimensional density of states ( $D \sim \omega$ ). Whereas, in the case of strongly bonded interfaces, the local density of states is similar to that of the bulk with an  $\omega^2$  relation that is characteristic to a three-dimensional solid.<sup>36,40</sup> Therefore, we note that a modification to the density of states in Eq. (5) could effectively account for the decrease in  $\alpha_T$  for the weakly bonded cases, which is beyond the scope of this study but offers a potential direction forward for analytical-based DMM approaches to capture bonding effects.

#### IV. SUMMARY

In summary, an analytical model for gas accommodation on solid surfaces based on diffuse mismatch theory is derived, which is used to calculate the equilibrium thermal accommodation coefficient at a solid/gas interface. We validate our analytical model by comparing the predictions to results obtained via molecular dynamics simulations. Our model is applicable for non-cryogenic temperatures and relatively strong solid-gas interactions ( $\varepsilon_{sf} \gtrsim k_B T$ ).

#### ACKNOWLEDGMENTS

We appreciate support from the Office of Naval Research (Grant No. N00014-15-12769).

<sup>1</sup>C. He, C. Liu, H. Gao, H. Xie, Y. Li, S. Wu, and J. Xu, *Energy* **38**, 136 (2012).

<sup>2</sup>X. Shi and D. Che, *Energy Convers. Manage.* **50**, 567 (2009).

<sup>3</sup>H. M. Hettiarachchi, M. Golubovic, W. M. Worek, and Y. Ikegami, *Energy* **32**, 1698 (2007).

<sup>4</sup>P. Zhao, L. Zhao, G. Ding, and C. Zhang, *Appl. Therm. Eng.* **22**, 1749 (2002).

<sup>5</sup>C. Oshman, Q. Li, L.-A. Liew, R. Yang, Y. C. Lee, V. M. Bright, D. J. Sharar, N. R. Jankowski, and B. C. Morgan, *J. Micromech. Microeng.* **22**, 045018 (2012).

<sup>6</sup>H. N. Chaudhry, B. R. Hughes, and S. A. Ghani, *Renewable Sustainable Energy Rev.* **16**, 2249 (2012).

<sup>7</sup>A. Faghri, *J. Heat Transfer* **134**, 123001 (2012).

<sup>8</sup>V. Bruch, "An assessment of research and development leadership in ocean energy technologies," Sandia National Laboratories Technical Report No. SAND-93-3946, 1994.

- <sup>9</sup>T. Hung, S. Wang, C. Kuo, B. Pei, and K. Tsai, *Energy* **35**, 1403 (2010).
- <sup>10</sup>L. Hu, T. Desai, and P. Keblinski, *Phys. Rev. B* **83**, 195423 (2011).
- <sup>11</sup>A. Reardon, *J. Low Temp. Phys.* **109**, 763 (1997).
- <sup>12</sup>G. A. Toombs and L. J. Challis, *J. Phys. C: Solid State Phys.* **4**, 1085 (1971).
- <sup>13</sup>G. A. Toombs and R. M. Bowley, *J. Phys. C: Solid State Phys.* **6**, L406 (1973).
- <sup>14</sup>E. T. Swartz and R. O. Pohl, *Rev. Mod. Phys.* **61**, 605 (1989).
- <sup>15</sup>P. Reddy, K. Castelino, and A. Majumdar, *Appl. Phys. Lett.* **87**, 211908 (2005).
- <sup>16</sup>R. Prasher, *Appl. Phys. Lett.* **94**, 041905 (2009).
- <sup>17</sup>P. E. Hopkins, J. C. Duda, and P. M. Norris, *J. Heat Transfer* **133**, 062401 (2011).
- <sup>18</sup>J. C. Duda, J. L. Smoyer, P. M. Norris, and P. E. Hopkins, *Appl. Phys. Lett.* **95**, 031912 (2009).
- <sup>19</sup>F. O. Goodman and H. Y. Wachman, *Dynamics of Gas-Surface Scattering* (Academic Press, New York, San Francisco, London, 1976).
- <sup>20</sup>Z. Liang, W. Evans, and P. Keblinski, *Phys. Rev. E* **87**, 022119 (2013).
- <sup>21</sup>Z. Liang, W. Evans, T. Desai, and P. Keblinski, *Appl. Phys. Lett.* **102**, 061907 (2013).
- <sup>22</sup>Z. Liang and P. Keblinski, *Int. J. Heat Mass Transfer* **78**, 161 (2014).
- <sup>23</sup>F. O. Goodman and H. Y. Wachman, *J. Chem. Phys.* **46**, 2376 (1967).
- <sup>24</sup>K. Daun, G. Smallwood, and F. Liu, *Appl. Phys. B* **94**, 39 (2009).
- <sup>25</sup>K. Daun, T. Sipkens, J. Titantah, and M. Karttunen, *Appl. Phys. B* **112**, 409 (2013).
- <sup>26</sup>R. Cheaito, J. T. Gaskins, M. E. Caplan, B. F. Donovan, B. M. Foley, A. Giri, J. C. Duda, C. J. Szejewski, C. Constantin, H. J. Brown-Shaklee, J. F. Ihlefeld, and P. E. Hopkins, *Phys. Rev. B* **91**, 035432 (2015).
- <sup>27</sup>J. C. Duda, T. E. Beechem, J. L. Smoyer, P. M. Norris, and P. E. Hopkins, *J. Appl. Phys.* **108**, 073515 (2010).
- <sup>28</sup>J. C. Duda, P. E. Hopkins, J. L. Smoyer, M. L. Bauer, T. S. English, C. B. Saltonstall, and P. M. Norris, *Nanoscale Microscale Thermophys. Eng.* **14**, 21 (2010).
- <sup>29</sup>W. G. Vincenti and C. H. Kruger, *Introduction to Physical Gas Dynamics* (R.E. Krieger, Malabar, FL, 1986).
- <sup>30</sup>J. W. Lynn, H. G. Smith, and R. M. Nicklow, *Phys. Rev. B* **8**, 3493 (1973).
- <sup>31</sup>P. M. Norris and P. E. Hopkins, *J. Heat Transfer* **131**, 043207 (2009).
- <sup>32</sup>D. W. Calvin and T. M. Reed, *J. Chem. Phys.* **54**, 3733 (1971).
- <sup>33</sup>Y. Chen, D. Li, J. Yang, Y. Wu, J. R. Lukes, and A. Majumdar, *Physica B* **349**, 270 (2004).
- <sup>34</sup>Y. Chen, D. Li, J. R. Lukes, Z. Ni, and M. Chen, *Phys. Rev. B* **72**, 174302 (2005).
- <sup>35</sup>J. Yu and H. Wang, *Int. J. Heat Mass Transfer* **55**, 1218 (2012).
- <sup>36</sup>J. C. Duda, T. S. English, E. S. Piekos, W. A. Soffa, L. V. Zhigilei, and P. E. Hopkins, *Phys. Rev. B* **84**, 193301 (2011).
- <sup>37</sup>W. G. Hoover, *Phys. Rev. A* **31**, 1695 (1985).
- <sup>38</sup>H. J. C. Berendsen, J. P. M. Postma, W. F. van Gunsteren, A. DiNola, and J. R. Haak, *J. Chem. Phys.* **81**, 3684 (1984).
- <sup>39</sup>F. Muller-Plathe, *J. Chem. Phys.* **106**, 6082 (1997).
- <sup>40</sup>A. Giri and P. E. Hopkins, *Appl. Phys. Lett.* **105**, 033106 (2014).